SCIENTIFIC REPORTS

OPEN

Ultraviolet light illuminates the avian nature of the Berlin *Archaeopteryx* skeleton

Received: 2 July 2018
Accepted: 22 November 2018
Published online: 24 April 2019

Daniela Schwarz[1], Martin Kundrát[2], Helmut Tischlinger[3], Gareth Dyke[2,4] & Ryan M. Carney[5]

The question of whether the iconic avialan *Archaeopteryx* was capable of active flapping flight or only passive gliding is still unresolved. This study contributes to this debate by reporting on two key aspects of this fossil that are visible under ultraviolet (UV) light. In contrast to previous studies, we show that most of the vertebral column of the Berlin *Archaeopteryx* possesses intraosseous pneumaticity, and that pneumatic structures also extend beyond the anterior thoracic vertebrae in other specimens of *Archaeopteryx*. With a minimum Pneumaticity Index (PI) of 0.39, *Archaeopteryx* had a much more lightweight skeleton than has been previously reported, comprising an air sac-driven respiratory system with the potential for a bird-like, high-performance metabolism. The neural spines of the 16th to 22nd presacral vertebrae in the Berlin *Archaeopteryx* are bridged by interspinal ossifications, and form a rigid notarium-like structure similar to the condition seen in modern birds. This reinforced vertebral column, combined with the extensive development of air sacs, suggests that *Archaeopteryx* was capable of flapping its wings for cursorial and/or aerial locomotion.

Living birds have extensively pneumatized postcrania, due to their unique and extremely efficient respiratory system[1,2]. This adaptation includes a series of pneumatic diverticula that derive from large air sacs, encompass the lungs, and invade different parts of the skeleton[3], leaving clear marks (pneumatic foramina) found in both avian and non-avian dinosaurs[4–6]. Reconstructions of pneumatic structures in fossil archosaurs have been previously based on comparisons with extant birds[1,2,5–8]. Evidence used to infer intraosseous pneumaticity for dinosaurs, in particular isolated foramina in compact bone or "blind" fossae, remains ambiguous however, as these cavities can house other structures such as muscles, fat, or neurovascular tissue[1]. The only unambiguous, reliable indicators of intraosseous pneumaticity are cortical foramina and communicating fossae connected with larger cavities within the bone[1]. Furthermore, the locations of foramina in the vertebrae or limb bones of dinosaurs that are comparable to those in extant birds support the interpretation of such structures as pneumatic[1,2,7]. The large cavities within pneumatic vertebrae of dinosaurs have been descriptively separated according to their architecture into larger and rounded camerae, and smaller and more angular-walled camellae[8–10]. Both types of internal pneumatic structures can occur in the same skeletal element, and multiple camellae can create a specific honeycomb-like pattern as in extant birds, described as somphospondylous[10]. The anteroposterior extension and spatial distribution of intraosseous pneumaticity provides critical anatomical evidence enabling reconstructions of the respiratory apparatus. The extent of pneumaticity also enables assessment of body weight, locomotor preferences, and metabolic activity, and therefore provides insights on the paleobiology and behavior of extinct animals[5–7].

In *Archaeopteryx*, both the presence and extent of intraosseous pneumaticity has been controversially discussed ever since the 19th century[11]. A recent microtomographic study on the Daiting specimen (*Archaeopteryx albersdoerferi*) showed that all cranial bones, shoulder girdles, and wing bones contain internal pneumatic cavities[12]. Similar observations have been based on the Berlin, London, and Eichstätt specimens, which preserve foramina on the surfaces of their presacral vertebrae and pubes[1,7,13–15]. Pneumatic foramina have been described in the 2nd to 5th cervical vertebrae[1,7,13,15] and posterior presacral vertebrae of the Berlin *Archaeopteryx*[16,17]; this specimen is also known to have hollow thoracic ribs[13]. The most unequivocal pneumatic structure seen in the

[1]Museum für Naturkunde, Leibniz Institute for Evolution and Biodiversity Science, 10115, Berlin, Germany. [2]Center for Interdisciplinary Biosciences, Technology and Innovation Park, University of Pavol Jozef Šafárik, 04154, Košice, Slovakia. [3]Tannenweg 16, 85134, Stammham, Germany. [4]Department of Geology, Babes-Bolyai University, Cluj-Napoca, Romania. [5]Department of Integrative Biology, University of South Florida, 33620, Tampa, FL, USA. Correspondence and requests for materials should be addressed to D.S. (email: daniela.schwarz@mfn.berlin) or M.K. (email: martin.kundrat@upjs.sk)

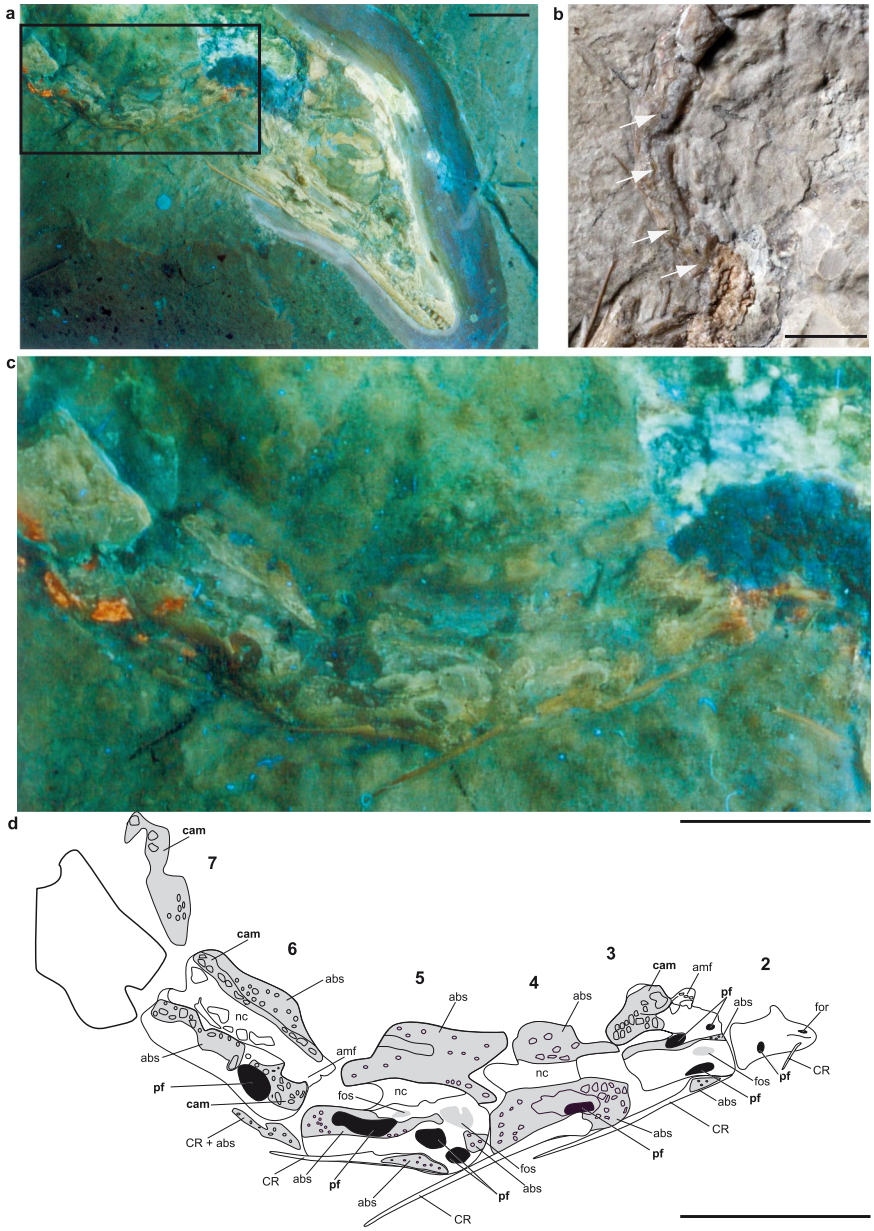

Figure 1. Photographs and interpretative drawing of cervical vertebrae of the Berlin specimen of *Archaeopteryx*, MB.Av.101. (**a**) UV photograph of the neck and skull, (**b**) photograph of the neck under visual light, structures previously described and figured[12] are marked, (**c**) magnified frame of (**a**) showing details of pneumatic structures in the neck, (**d**) interpretative drawing of (**c**) with recognized pneumatic structures. Anatomical abbreviations used: abs, area of abraded bone surface with regular spongy internal structure; amf, area with unidentified pores or putative camellae; cam, pneumatic camellae; CR, cervical rib; for, foramen; fos, fossa; nc, neural canal; pf, pneumatic foramen. Pneumatic foramina and camellae are unambiguous pneumatic structures and labeled with bold face. Foramina and pneumatic foramina are filled with black; fossae are filled with grey but without margin. Scale bars are 10 mm.

postcranial skeleton of the Berlin specimen is the pneumatic foramen in the body of the 5th cervical vertebra[1], exemplifying the 'common pattern' seen in earlier-diverging theropod dinosaurs[7].

Here, we describe intact and incomplete postcranial bone surfaces in the Berlin *Archaeopteryx* (MB.Av.101; MB = Museum Berlin, Av = Collection of fossil birds), utilizing long-wave UV light[15,18] to reveal pneumatic structures that are hidden, or difficult to discern, under visible light conditions (Fig. 1). Previous work has shown that UV light is far more sensitive than visible light to the increased contrast between fossilized bone, rocky infill, and surrounding matrix[15,18–21]. A previous description based on UV observations of the Berlin *Archaeopteryx* (MB.Av.101)[15] has corroborated other reports[1,13] regarding the presence of pneumatic foramina in the cervical vertebral column and hollow vertebral bodies for the 7th to 10th presacral vertebrae. The new UV findings we present here extend these results, enable a detailed account of all unambiguous pneumatic structures in the postcranial

skeleton of MB.Av.101, and confirm that numerous postcranial bones of *Archaeopteryx* were reduced in mass via hollow interiors (Table S1).

Results

In the Berlin *Archaeopteryx*, the vertebral cortex has been abraded in most presacral vertebrae, possibly due to repeated preparation[15,18], exposing the internal bone structure of the vertebrae and ribs. UV light conditions expose pneumatic structures more clearly than under visible light, and reveal a far more extensive distribution of intraosseous pneumaticity than has been described since the 19th century. Sharp-lipped pneumatic foramina, which are distinguished from nutrient foramina by their larger diameter[13], are present at the vertebral body and neural arch of the 2nd to 5th cervical vertebrae, as reported before[1,13,15]. Pneumatic foramina can also be identified on the 6th, 16th, and 22nd presacral vertebrae (Figs 1 and 2, Table S1). In the 19th presacral vertebra, a combination of a fossa with a communicating foramen is visible at the vertebral body (Fig. 2d). In contrast, small foramina visible in most of the vertebrae likely represent nutrient foramina, and are therefore not evidence for intraosseous pneumaticity[1,13]. In the 8th to 14th presacral vertebrae (Fig. 2), and the 1st to 3rd, 12th, and 14th to 16th caudal vertebrae (Fig. 3), the interiors exhibit large internal pneumatic chambers, or camerae. The 3rd, 8th to 14th, 16th, and 20th presacral vertebrae, and the 2nd, 5th, 6th and 11th caudal vertebrae expose pneumatic camellae. These camellae are small, sometimes rounded but mostly angular voids, separated from each other by thin bone walls (Figs 1 and 2b,c); they form a characteristic honeycomb-like pattern that can also be observed in the pneumatic vertebrae of extant birds[1]. In most vertebrae, the camellae are combined with unambiguous pneumatic foramina and large internal camerae (Table S1) typical for pneumatized bones, and are more often preserved in the neural arches than in the vertebral bodies.

At the vertebral bodies, the abraded cortical bone exposes an internal structure that consists of regular, small, and mostly oval pores that are only half as large as the camellae (abs). Rounded and irregularly distributed voids the same size as camellae are visible (amf) in other areas, mostly along the neural arches and in particular all presacral vertebrae and the 3rd and 6th to 8th caudal vertebra (Fig. 1–3). These structures cannot be unambiguously identified as pneumatic structures, as they do not correspond to a typical camellate pattern as described above, but might instead represent areas of spongy bone. The presence of spongy internal bone structure can be taken as evidence for lightweight vertebrae in MB.Av.101. The thoracic ribs also exhibit a pattern comprising small regular and irregular voids in their heads and along their shafts, while their internal shafts are hollow[13] (Fig. 2a,d; Table S1). A pattern of small and irregular pores can be observed in the posterior process and ventral margin of the ilium, and the head of the pubis (Fig. 3). Only small putative nutrient foramina are observed within the humerus, pelvic bones, femur, and tibia (Figs 2a,d and 3a, Table S1), so unambiguous evidence for intraosseous pneumaticity in the appendicular skeleton is still unknown[1,8].

The overall skeletal pneumaticity in *Archaeopteryx* was calculated using the Pneumaticity Index (PI), as it provides a quantitative measure for the standardized comparison of postcranial pneumaticity among multiple avian species, independent of phylogeny, body size, and behavior[22]. Mapping of intraosseous pneumaticity in the Berlin *Archaeopteryx* yielded a PI of at minimum 0.39 (7 of 18 anatomical units being pneumatic). This value is comparable to the PI of a few of the extant anseriform birds previously reported, such as *Mergus merganser* and *Anas georgica*[22] (both 0.41).

Our UV light observations also corroborate the presence of a notarium-like structure of fused presacral vertebrae in the Berlin *Archaeopteryx*. Fused anterior thoracic vertebrae have been mentioned briefly before[23], but never described in detail. Our images reveal the presence of a massive, rod-shaped ossification above the apex of the 16th presacral neural spine and connecting to the anterior spine of the 17th (Fig. 4a,b). The caudodorsal corner of the 17th neural spine and the craniodorsal corner of its 18th counterpart comprise a long, thin, rod-like structure that bridges and tightly binds the neural spines together (Fig. 4a,b). The neural spines of the 19th to 20th presacral vertebrae are equally drawn out in their anterodorsal and posterodorsal corners, and fused dorsally with their adjacent neural spines. However, the connection between these elements is partly broken (Fig. 4a,b), while the neural spine of the 21st presacral vertebra has extended anterodorsal and posterodorsal corners.

Discussion

It is generally accepted that the clearest marker of skeletal pneumaticity is the presence of intraosseous pneumatic structures correlated with foramina[1,7,24]. Hitherto, the presacral distribution of pneumatic structures in *Archaeopteryx* has been discussed solely on the basis of described pneumatic foramina, which is considered controversial[1,7]. Previous workers have noted the existence of such pneumatic foramina on the surfaces of the cervical and thoracic vertebrae, humerus, and pubis of the Berlin, London, Eichstätt, and Thermopolis specimens of *Archaeopteryx*[1,7,8,12–17,25] (Table S2). However, the most recent integrative study concluded that just the cervical and anteriormost thoracic vertebrae were pneumatized in *Archaeopteryx*, analogous with the plesiomorphic 'common pattern' seen in basal theropod dinosaurs[7]. In this study, we expand our knowledge of the Berlin *Archaeopteryx* with the first evidence of unambiguous intraosseous pneumatic structures (i.e., internal cavities such as camerae and camellae). The UV findings now enable convincing identification of internally pneumatic presacral vertebrae (2nd to 14th, 16th, 20th, 22nd) and caudal vertebrae (1st to 3rd, 5th, 6th, 11th, 12th, 14th to 16th), demonstrating the extension of pneumatic foramina and intraosseous pneumatic structures to most the vertebral column. Unambiguous traces of vertebral pneumaticity are absent in the remaining thoracic vertebrae, which is consistent with other specimens of *Archaeopteryx*[1,7,13,14,26]. The thoracic ribs are hollow, which has also been reported for the12th specimen of *Archaeopteryx*[26]. The presence of intraosseous pneumaticity in the remaining caudal vertebrae remains unclear, due to the lack of a combination of unambiguous pneumatic structures. We found evidence for at least a spongy and therefore light bone architecture in the 1st and 2nd sacral vertebra, the ilium and the pubis, as well as in some other caudal vertebrae (Fig. 3).

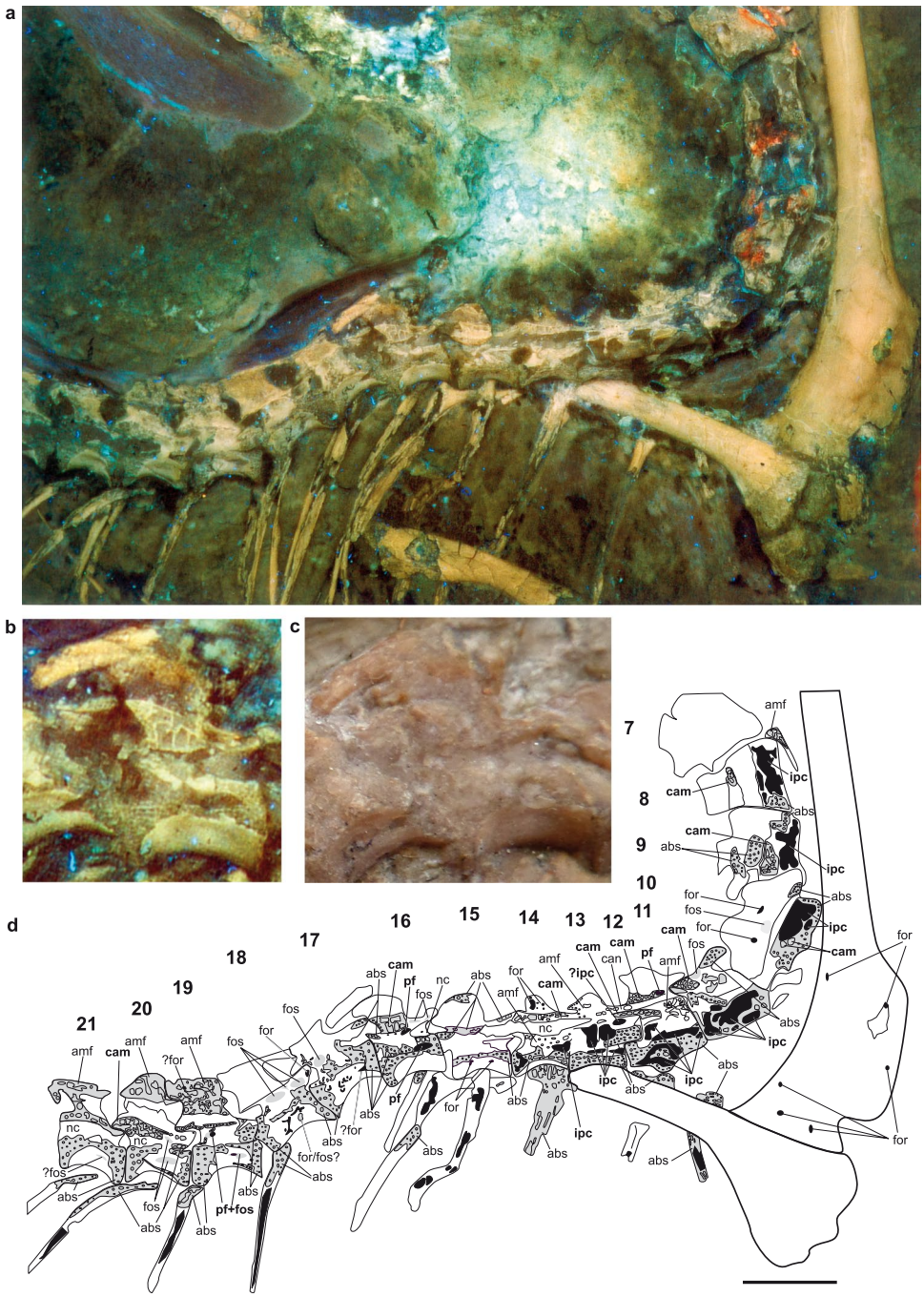

Figure 2. Photographs and interpretative drawing of presacral (thoracic) vertebrae with pneumatic structures of the Berlin specimen of *Archaeopteryx*, MB.Av.101. (**a**) UV photograph, (**b**) magnification of 16th presacral vertebra under UV light, and (**c**) the same vertebra under visible light, (**d**) interpretative drawing of region a. Anatomical abbreviations used: abs, area of abraded bone surface with regular spongy internal structure; amf, area with unidentified pores or putative camellae; cam, pneumatic camellae; for, foramen; fos, fossa; ipc, internal pneumatic camerae; nc, neural canal; pf, pneumatic foramen. Pneumatic foramina, internal camerae and camellae are unambiguous pneumatic structures and labeled with bold face. Foramina and pneumatic foramina are filled with black; fossae are filled with grey but without margin. Scale bars are 10 mm.

Our survey revealed furthermore that the abraded and broken lumbar vertebra of the Maxberg specimen[27] also includes a pneumatized internal vertebral body including camellae (Table S2). Additionally, X-ray images of the thoracic vertebrae of the Maxberg *Archaeopteryx*[27] and the cervicals of the Thermopolis specimen[25] corroborate the presence of camellae within these vertebrae (Table S2). Additionally, camellate intraosseous pneumatic structures in the last two cervical vertebrae, as well as a pneumatic foramen in the 1st thoracic vertebra (Rauhut *et al*. 2018, p.30; Fig. 17), have been described for the most recently reported 12th specimen of *Archaeopteryx*[26]. Therefore, the presence of intraosseous postcranial pneumaticity in at least four specimens of *Archaeopteryx*

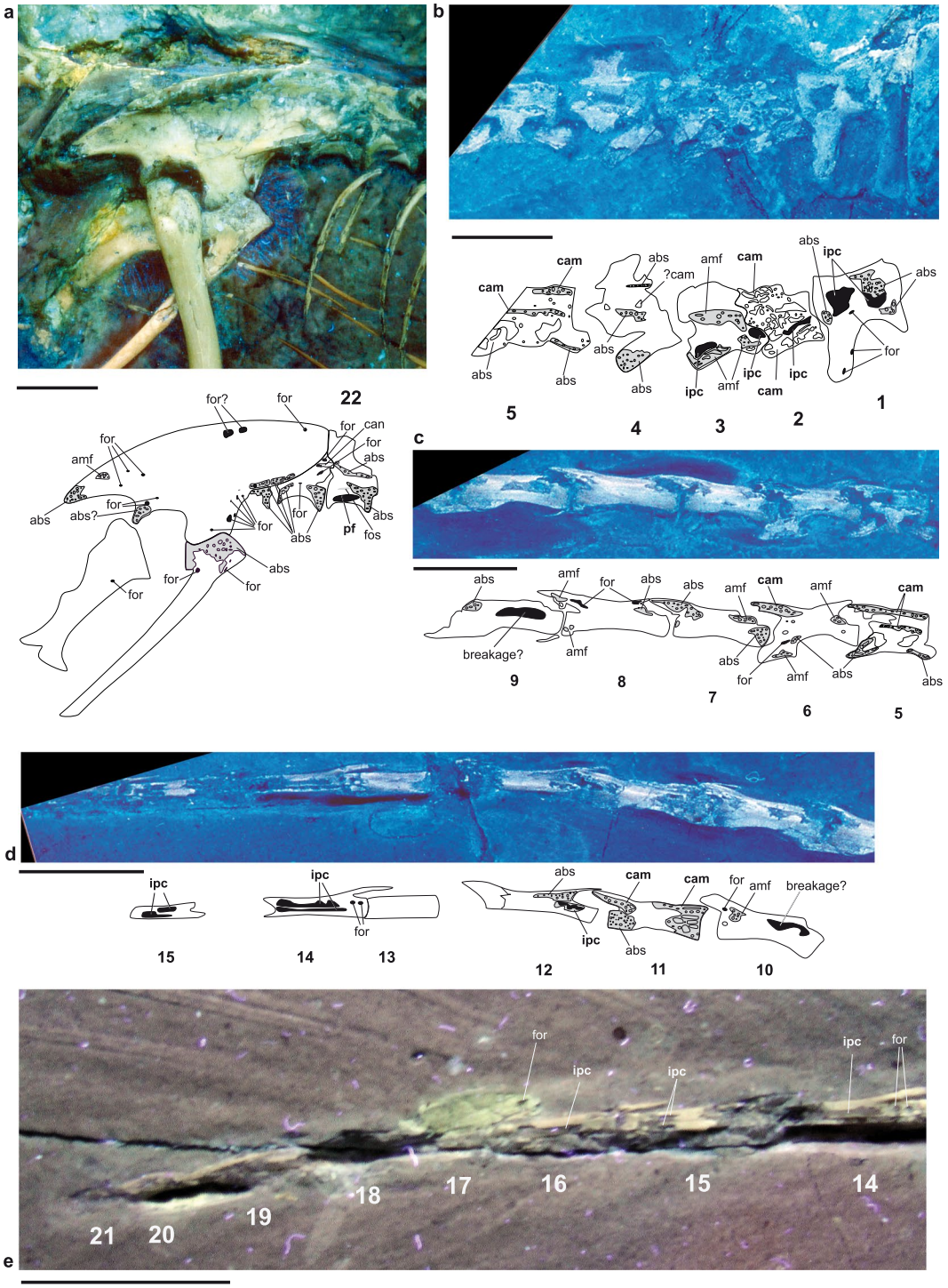

Figure 3. UV photographs and interpretative drawings of the pelvis and sacral and caudal vertebrae with pneumatic structures of the Berlin specimen of *Archaeopteryx*, MB.Av.101. (**a**) Pelvic region in lateral view, with the last (22nd) presacral vertebra, (**b**) 1st to 5th caudal vertebra, (**c**) 5th to 9th caudal vertebrae, (**d**) 10th to 15th caudal vertebrae, (**e**) 14th to 21st (last) caudal vertebrae. Anatomical abbreviations and filling of structures as in Figs 1 and 2. Scale bars are 10 mm.

including the Berlin, Maxberg, Thermopolis, and the 12th specimen, is documented (Table S2). At least in two specimens, the Maxberg and the Berlin *Archaeopteryx*, pneumatic structures extend outside the region of the anterior thoracic vertebrae. A hollow caudal vertebra is described for the 12th *Archaeopteryx*[26], although it is unclear whether this represents intraosseous pneumaticity. Clearly seen in the Berlin *Archaeopteryx*, the pattern of intraosseous pneumaticity comprises a combination of closely-spaced honeycomb-shaped camellae bounded by thin bone walls (Fig. 2b), essentially similar to that of extant birds[1,6,8,10]. Camellate pneumatic bone is also

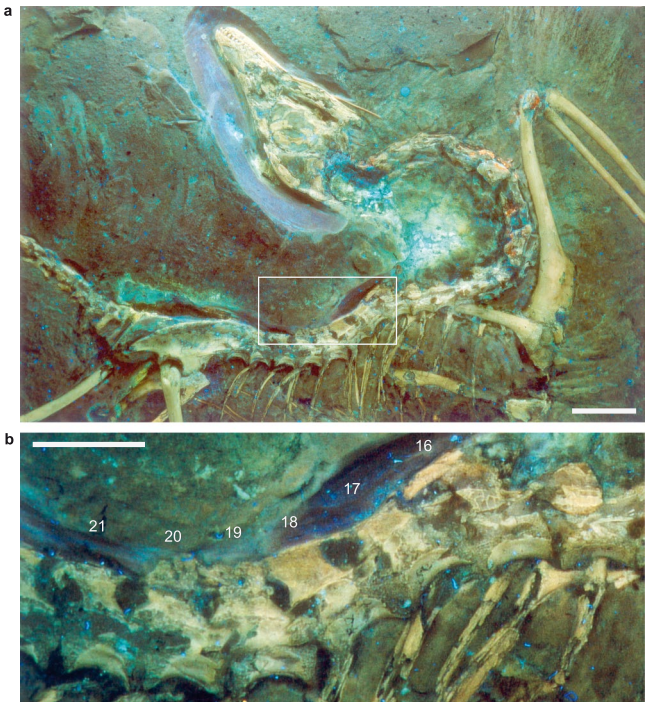

Figure 4. UV photographs of the Berlin specimen of *Archaeopteryx*, MB.Av.101, with magnified region of the fused presacral neural spines forming a notarium-like structure. (**a**) Axial skeleton of *Archaeopteryx*, white frame demarks area of fused neural spines; scale bar is 20 mm. (**b**) Magnification of the 16th to 22nd presacral vertebrae, white arrows mark ossifications between the neural spines and remnants of broken spinal processes; scale bar is 10 mm.

found in a range of non-avialan dinosaurs (e.g. *Aerosteon*[28], *Tyrannosaurus*[29], and other neotheropods[8]) and in the avialan *Rahonavis*[30], whereas large internal pneumatic camerae have been less frequently reported (e.g., in megalosauroids[31], dromaeosaurids[8] and ornithomimosaurs[32]).

Our new data demonstrate that the pneumaticity status of *Archaeopteryx* does not, in fact, conform to the plesiomorphic "common pattern" of non-avialan theropod dinosaurs[7]. Instead, *Archaeopteryx* possesses what can be termed "extended pattern of pneumaticity" (EPP)[7], which includes the posterior thoracic vertebrae, and at least some anterior caudal vertebrae. The EPP is also seen in basal Neotheropoda[6,7], as well as in most neotheropod clades, including Tyrannosauroidea[28], Oviraptorosauria[33–35], Dromaeosauridae[36], and Troodontidae[37,38], where it is thought to have evolved independently[7]. Among Maniraptora, only Oviraptorosauria possesses a stronger pneumatized vertebral column, including the complete tail[39]. Apart from *Archaeopteryx*, evidence of postcranial pneumaticity within Avialae is patchy, possibly related to the small body size and fragmentary preservation of most specimens. Pneumatic foramina are documented for the cervical vertebrae of confuciusornithid birds[40], and for the cervical and anterior thoracic vertebrae of *Rahonavis* and some enantiornithid birds[30], which would conform to a "common pattern" of intraosseous pneumaticity. One report of a pneumatic foramen in the humerus of an enantiornithid bird[41] might indicate an EPP, but the evolutionary development of this pattern within Avialae still remains unclear. In any case, the level of pneumaticity we found in *Archaeopteryx* already corresponds with the EPP seen in some extant neornithine birds, including non-diving anseriforms[22].

The new evidence of intraosseous pneumatization in *Archaeopteryx* presented here indicates that the respiratory system of this avialan included an air sac distribution similar to that of living birds[1,3,6,22] (Table S1). The extensive intraosseous postcranial pneumatic structures provide unambiguous evidence for the presence of cervical air sacs that pneumatize cervical vertebrae and ribs, as well as anterior to mid-thoracic vertebrae and thoracic ribs. Intraosseous pneumatization of the mid- to posterior thoracic and caudal vertebrae provide unambiguous evidence for the existence of abdominal air sacs[1,3,22] (Fig. 5). There is no osteological evidence for the presence of clavicular and anterior thoracic air sacs surrounding the lungs, which would pneumatize the humerus[22] (Fig. 2, Table S1). The exact position of the lungs also cannot be reconstructed, because this organ is not associated with osteological traces; the lack of pulmonary foramina in thoracic vertebrae of *Archaeopteryx* makes it unlikely that lung tissue pneumatized these vertebrae on a large scale[1]. Similarly, the presence of posterior thoracic air sacs, present in extant birds, cannot be reconstructed for *Archaeopteryx* because these air sacs do not pneumatize the skeleton[1,3,22]. The reconstruction of air sacs in *Archaeopteryx* (Fig. 5) confirms the already assumed[1,7] presence of a bird-like, high-compliance lung-air sac respiration system, incorporating lungs fixed at the rigid thoracic vertebral column and ventilated by air sacs positioned anteriorly and posteriorly to it.

The rostrad extension of skeletal pneumatization in theropod dinosaurs is a "centrum-first" pattern[7], which means that first the vertebral bodies are pneumatized via pneumatic foramina ("intramural pneumatization")[42], followed by the neural arches. This is consistent with the occurrence of pneumatic foramina throughout the

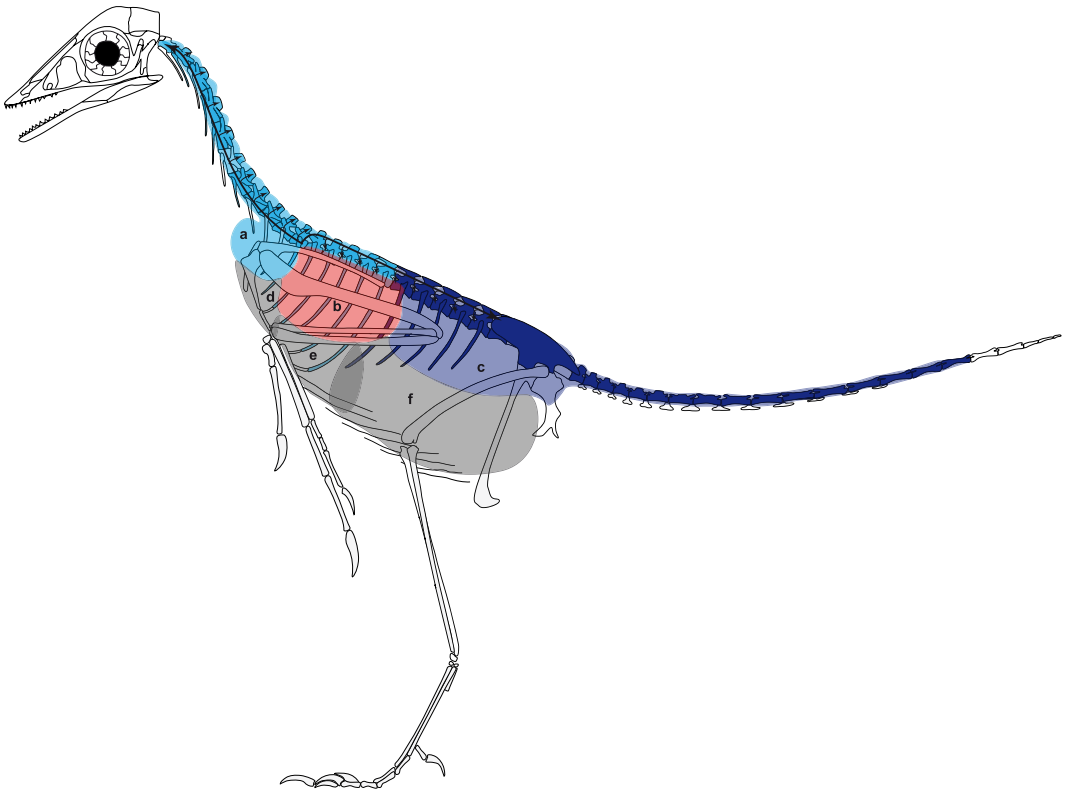

Figure 5. Skeleton of *Archaeopteryx* (Berlin specimen, MB.Av.101) with schematic representation of air sacs and pneumatic postcranial elements as deduced from this study. Skeleton is shown from left lateral side and paired elements are represented only from the left body side. Black arrows indicate the path of pneumatization within air sacs. Light blue = cervical air sac (**a**), red = lung (**b**), dark blue = abdominal air sac (**c**). Grey = clavicular (**d**), anterior thoracic (**e**), and posterior thoracic (**f**) air sacs; these have no osteological evidence in *Archaeopteryx*, making their presence uncertain. Skeleton redrawn from Wellnhofer[26].

cervical vertebral column of the Berlin specimen (Fig. 1). In the posterior direction, pneumatization proceeds in a "neural arch-first" pattern, with the neural arches being pneumatized first, followed by pneumatization of the vertebral bodies[1,7]. Pneumatic diverticula can proceed through the medullary region first, and enter the vertebral body internally, as in extant birds[1,10,43]. This pattern likely explains the lack of pneumatic foramina observed in the thoracic vertebral bodies in *Archaeopteryx* (Fig. 2), which contrasts its rich intraosseous pneumatic structures. Such an absence of pneumatic foramina in the mid- thoracic region is consistent with many extant birds, in which pneumatic foramina are reduced in the thoracic vertebral series towards the sacrum[1].

Pneumatization of the postcranial skeleton has a direct weight-reducing effect, by replacing bone and marrow with air-filled cavities[42,44,45]. A correlation between the degree of vertebral pneumaticity and body size was found in large-bodied, non-avian theropod dinosaurs[7]. In extant birds, the degree of postcranial pneumaticity has traditionally been linked to body mass and diving behavior, with the assumption that larger-bodied birds are more pneumatic than smaller-bodied birds, and the known absence of intraosseous pneumaticity in diving birds such as penguins[22]. At least within anseriform birds, no statistically significant relationships between body size and Pneumaticity Index has been found[22], so that reduced or absent intraosseous pneumaticity (such as in diving taxa) seems not to be generally correlated with the absence of active flight. In smaller extant birds, the threshold of a critical body mass related to the energetic requirements of flight is not reached by a reduction or increase of intraosseous pneumaticity, meaning that the amount, presence, or absence of postcranial intraosseous pneumaticity gives no information on the flight capability of an extant bird[22]. However, if the metabolic activity of a fossil avialan such as *Archaeopteryx* was different than that of extant birds, then the increase of intraosseous pneumaticity might very well have had an effect on the critical body mass, and thereby also the flight capability in *Archaeopteryx*. Nevertheless, given the remaining uncertainty in the reconstruction of both the total extension of postcranial intraosseous pneumaticity and the presence of all pulmonary air-sacs, the precise estimation of body mass in *Archaeopteryx* remains speculative. A hypothetical adult (somatically mature) *Archaeopteryx* has been reconstructed to exceed 500 mm in body length and have a body mass between 0.8 and 1 kg, comparable to a raven (*Corvus corax*)[46], values which we assume to be within the possible ranges for this taxon and not contradicted by the new data on intraosseous pneumaticity in this study.

The documentation of stiffening structures in neural spines of the thoracic vertebral column of *Archaeopteryx* is rather novel, and we argue that these ossifications represent the earliest known occurrence of a notarium-like structure on the line to extant birds, pushing back its origin to Paraves. Previously, spinal processes in the thoracic vertebrae had only been described in late Cretaceous enantiornithine birds[41]. It is also

interesting to note the absence of stabilization structures in basal birds more derived than *Archaeopteryx*, such as the Confuciusornithidae, as well as the heterogeneous distribution of notaria in extant birds[47–51]. The apparent absence of these structures in other specimens of *Archaeopteryx* must remain speculative, and might be due to differing degrees of tendon ossification and/or preservation in these specimens. In several members of extant avian groups such as Tinamiformes, Podicipediformes, Phoenicopteriformes, Galliformes, Columbiformes, Pelecaniformes, Falconiformes, Gruiformes, and Caprimulgiformes, the vertebrae of the thorax form a notarium; this is a rigid structure created by 2–5 ankylosed vertebrae, including ossified tendons and ligaments, and separated in most cases from the synsacrum by at least one "free" or unankylosed vertebra[47–51]. Importantly, the fusion of neural spines in *Archaeopteryx* lies in the thoracic vertebral column between the 16th and the 22nd presacral vertebrae (Fig. 4a,b), corresponding to the notarium region in extant avians[51], and there is also a vertebral gap between the fused and sacral regions. The narrow, 'rod-like structures along the neural spines are interpreted to represent ossified ligaments[52] or tendons of the epaxial trunk musculature. These would have acted as bony splints[52], and likely contributed to an incipient ankylosis between the vertebrae (although the vertebral bodies themselves are not fused with each other).

A relatively rigid thoracic vertebral column is required for a bird-like respiration mechanism[3], and is therefore an important structure to be documented in *Archaeopteryx*. In extant birds, the biological importance of the notarium is explained mostly as a rigid stabilization structure, counteracting mechanical stress occurring during wing-driven flapping flight and acting as a shock absorber during landing[50]. A notarium has also been described for some pterosaurs as an adaptation to active flight[53,54]. In any case, fusion of the neural spines creates a more stable (but less flexible) region in the vertebral column, which acts as a unit and can be more effectively stabilized by the available muscles and ligaments against the mechanical forces during locomotion.

Ultimately, reinforcement structures in the thoracic vertebral column can be interpreted to facilitate novel locomotor modes, in particular the development of active flapping flight or bipedal running supported by flapping wings, that increases stresses acting on the vertebral column. There has been controversial anatomical evidence on the ability of *Archaeopteryx* for gliding or flapping flight[27,55–59]. Nevertheless, the reinforcement structures observed in the trunk is indirect evidence for the increased use of forelimbs in *Archaeopteryx*, and depicts a stabilization trend that continues on the line to extant birds with the reduction in the number and increasing intervertebral fusion of thoracic vertebrae into a regional notarium[47,48,52].

Conclusions

We demonstrate that *Archaeopteryx* possessed a derived, bird-like postcranial pneumatization pattern that comprises intraosseous pneumatic camellae and camerae within the presacral vertebral column and caudal vertebrae. The new observations furthermore confirm that expanded postcranial pneumatic structures and a bird-like respiratory system, both important physiological adaptations for powered flight, were present in *Archaeopteryx*. Whereas the number of pneumatic bones has a direct effect on weight reduction in large-bodied dinosaurs[5,7], the camerate and camellate architecture of pneumatized bone is more likely determined by mechanical factors in the vertebral column, in concert with the evolutionary development and phylogenetic integration of the taxa. In *Archaeopteryx*, the direct effect on weight-reduction of the vertebral column by intraosseous pneumatic structures was moderate. As an indirect effect, the lightened pneumatic vertebral column would have needed less muscle forces to be stabilized against the mechanical loads that occur during all locomotor modes. Intraosseous pneumatization in *Archaeopteryx* was important for the metabolism of the animal, because the pneumatic epithelium replaces metabolically costly and massive bone, which reduces metabolic energy consumption and locomotion costs, and helped to increase the metabolic performance of the animal[7,45,59,60]. The putative high energetic advantage of a pneumatic postcranium[7,24] demonstrates the particular importance for a correct establishment of the pneumaticity status in *Archaeopteryx*. The presence of an expanded pneumatization pattern in *Archaeopteryx* indicates facilitation of an active lifestyle[7,12] and allows characterizing *Archaeopteryx* as a taxon that already had the metabolic prerequisites for this highly demanding active lifestyle and an avian-like, high-performance endothermy. The presence of a notarium-like stabilizing structure in the vertebral column in *Archaeopteryx* is fully in line with the new evidence on its expanded pneumaticity pattern, and adds another piece of evidence for the potential of this taxon for active, wing-driven flapping flight.

Methods

The main slab of the Berlin specimen of *Archaeopteryx*, MB.Av.101, was observed directly (by the naked eye) and with microscopy. The images taken by Helmut Tischlinger with the help of longwave UV light (365–366 nm) in combination with selective filter techniques[15,21] were examined carefully and compared to the original specimen. The UV photographs are available at the MfN. Additionally, new photographs under longwave UV radiation were taken by M.K. to supplement the older images and compare both of them. Comparative photographs under visible light were provided by R.C.

A survey of other described specimens of *Archaeopteryx* has been done mainly by literature to get an idea of potentially preserved pneumatic structures. The Maxberg specimen of *Archaeopteryx* is lost and therefore could only be examined by photographs from Wellnhofer[27]. Data on the Thermopolis specimen of *Archaeopteryx* were taken from Mayr *et al.*[25].

We assume that the first preserved vertebra visible in the head region represents the 2nd cervical because of its integration with the occiput; thus, the first vertebra with a thoracic rib is the 11th presacral vertebra (which has its rib slightly caudoventrally emplaced beneath the scapula), and so the first sacral vertebra (the rostralmost vertebra without a thoracic rib) is medial to the anterior iliac blade. We count therefore 22 presacral vertebrae in this specimen (i.e., 10 cervicals, and 12 rib-bearing thoracic vertebrae), one less than in the other known specimens of *Archaeopteryx*[14,27].

We calculated a Pneumaticity Index[22] (PI) as a quantitative measure to compare the amount of pneumatic elements throughout the postcranial skeleton with some extant birds. The PI is defined as the ratio between the number of pneumatic postcranial elements and the total number of postcranial elements[22]. Postcranial elements are subdivided into anatomical units (AU), yielding the equation of PI = #AU pneumatic/#AU total. The following AUs (see also Table S3) were defined for *Archaeopteryx:* Composite units = **ANC**, Anterior Cervical Vertebrae (1^{st} to 3^{th} cervical); **MC**, Middle Cervical Vertebrae (4^{th} to 6^{th} cervical); **POC**, Posterior Cervical Vertebrae (7^{th} to 10^{th} cervical); **ANT**, Anterior Thoracic Vertebra (1^{st} to 6^{th} thoracic); **POT**, Posterior Thoracic Vertebrae (7^{th} to 12^{th} thoracic); **SS**, Synsacral Vertebrae; **CAA**, Anterior Caudal Vertebrae; **CAP**, Posterior Caudal Vertebrae; **TR**, Thoracic Ribs; **CAR**, Caudal Ribs and Chevrons; **PE**, Pelvis (Ilium, Ischium, Pubis); **DFL**, distal forelimb elements (i.e., bones distal to elbow joints); **DHL**, distal hind limb elements (i.e., bones distal to knee joints); Individually scored units = **CC**, coracoids; **FU**, furculae; **FM**, femora; **HU**, humeri; **SC**, scapulae. In the Berlin specimen of *Archaeopteryx*, 7 (ANC, MC, POC, ANT, POT, CAA, TR) of the listed 18 AUs are unambiguously pneumatic, yielding a minimum **PI of 7:18 = 0.39**.

Data Availability

The original Berlin specimen of *Archaeopteryx*, MB.Av.101, is housed in the collection of fossil vertebrates at the Museum für Naturkunde in Berlin (MfN) and can be studied upon request at the institution. The authors declare that the data supporting the findings of this study are available within the paper and its supplementary information files.

References

1. O'Connor, M. P. Postcranial pneumaticity: An evaluation of soft-tissue influences on the postcranial skeleton and the reconstruction of pulmonary anatomy in archosaurs. *J. Morphol.* **267**, 1199 (2006).
2. O'Connor, M. P. The postcranial axial skeleton of *Majungasaurus crenatissimus* (Theropoda: Abelisauridae) from the Late Cretaceous of Madagascar. *Soc. Vertebr. Paleontol. Mem.* **8**(27), 127 (2007).
3. Duncker, H.-R. The lung air sac system of birds. *Adv. Anat. Embryol. Cel.* **45**, 1 (1971).
4. Perry, S. F. Method for reconstructing the respiratory system of extinct animals. *Sauropod dinosaurs as a case in point. Comp. Biochem. Physiol. A* **143**, 61 (2006).
5. Wedel, M. J. Vertebral pneumaticity, air sacs, and the physiology of sauropod dinosaurs. *Paleobiology* **29**, 243 (2003).
6. O'Connor, M. P. & Claessens, L. P. A. M. Basic avian pulmonary design and flow-through ventilation in nonavian theropod dinosaurs. *Nature* **436**, 253 (2005).
7. Benson, R. B. J., Butler, R. J., Carrano, M. T. & O'Connor, M. P. Air-filled postcranial bones in theropod dinosaurs: physiological implications and the 'reptile'–bird transition. *Biol. Rev.* **87**, 168 (2012).
8. B. B. Britt Thesis, University of Calgary (1993).
9. Wedel, M. J., Cifelli, R. I. & Sanders, R. K. Osteology, paleobiology, and relationships of the sauropod dinosaur. *Sauroposeidon. Acta Palaeontol. Pol.* **45**, 343 (2000).
10. Wedel, M. J. The evolution of vertebral pneumaticity in sauropod dinosaurs. *J. Vertebr. Paleontol.* **23**, 344 (2003).
11. Owen, R. On the *Archaeopteryx* of von Meyer, with a description of a new long tailed species from the lithographic stone of Solenhofen. *Philosophical Transactions of the Royal Society of London* **153**, 33 (1864).
12. Kundrát, M., Nudds, M. J., Kear, B., Lü, J. & Ahlberg., P. The first specimen of *Archaeopteryx* from the Upper Jurassic Mörnsheim Formation of Germany. Historical. *Biology* **1**, 3 (2018).
13. Britt, B. B., Makovicky, P. J., Gauthier, J. & Bonde, N. Postcranial pneumatization in *Archaeopteryx*. *Nature* **395**, 374 (1998).
14. Christiansen, P. & Bonde, N. Axial and appendicular pneumaticity in *Archaeopteryx*. *Proc. Roy. Soc. Lond., Series B* **267**, 2501 (2000).
15. Tischlinger, H. & Unwin, D. M. UV-Untersuchungen des Berliner Exemplars von *Archaeopteryx lithographica* H. v. MEYER 1961 und der isolierten Archaeopteryx-Feder. *Archaeopteryx* **22**, 17 (2004).
16. Ostrom, J. H. *Archaeopteryx* and the origin of birds. *Biological Journal of the Linnean Society* **8**, 91 (1976).
17. Elzanowski, A. In *Mesozoic Birds: Above the Heads of Dinosaurs*, Chiappe, L. & Witmer, L. M., Eds (University of California Press), pp. 129–159 (2002).
18. Tischlinger, H. Neue Informationen zum Berliner Exemplar von *Archaeopteryx lithographica* H.v.Meyer 1861. New information regarding the Berlin example of Archaeopteryx lithographica H.v.Meyer 1861. *Archaeopteryx* **23**, 33–50 (2005).
19. Hone, D. W. E., Tischlinger, H., Xu, X. & Zhang, F. The extent of the preserved feathers on the four-winged dinosaur *Microraptor gui* under ultraviolet light. *PLoS One* **5**, 1 (2010).
20. Rauhut, O. W. M., Foth, C., Tischlinger, H. & Norell, M. A. Exceptionally preserved juvenile megalosauroid theropod dinosaur with filamentous integument from the Late Jurassic of Germany. *PNAS* **109**, 11746–11751 (2012).
21. Tischlinger, H. & Arratia, G. Ultraviolet light as a tool for investigating Mesozoic fishes, with a focus on the ichthyofauna of the Solnhofen archipelago. in Mesozoic Fishes 5 – Global Diversity and Evolution, Arratia, G., Schultze, H.-P. & Wilson, H., Eds (Verlag Dr. Friedrich Pfeil, München), pp. 549–560 (2013).
22. O'Connor, M. P. Pulmonary pneumaticity in the postcranial skeleton of extant Aves: a case study examining Anseriformes. *J. Morphol.* **261**, 141 (2004).
23. Martin, L. D. The beginning of the modern avian radiation. Documents des Laboratoires de. *Geologie de la Faculte des Sciences de Lyon* **99**, 9–19 (1987).
24. O'Connor, M. P. Evolution of archosaurian body plans: Skeletal adaptations of an air-sac-based breathing apparatus in birds and other archosaurs. *J. Exp. Zool.* **311A**, 629 (2009).
25. Mayr, G., Pohl, B., Hartman, S. & Peters, D. S. The tenth skeletal specimen of *Archaeopteryx*. *Zool. J. Linn. Soc.* **149**, 97 (2007).
26. Rauhut, O. W. M., Foth, C. & Tischlinger, H. The oldest *Archaeopteryx* (Theropoda: Avialae): a new specimen from the Kimmeridgian/Tithonian boundary of Schamhaupten, Bavaria. *PeerJ* **6**, e4191 (2018).
27. Wellnhofer, P. *Archaeopteryx*. Der Urvogel von Solnhofen. (Verlag Dr. Friedrich Pfeil, München), pp. 256 (2008).
28. Sereno, P. C. *et al*. Evidence for avian intrathoracic air sacs in a new predatory dinosaur from Argentina. *PLoS One* **3**, e3303 (2008).
29. Brochu, C. A. Osteology of *Tyrannosaurus rex*: insights from a nearly complete skeleton and highresolution computed tomographic analysis of the skull. *Soc. Vertebr. Paleontol. Mem.* **7**(22), 1 (2002).
30. Forster, C. A., Sampson, S. D., Chiappe, L. M. & Krause, D. W. The theropod ancestry of birds: New Evidence from the Late Cretaceous of Madagascar. *Science* **279**, 1915 (1998).
31. Ewers, S. W., Rauhut, O. W. M., Milner, A. C., McFeeters, B. & Allain, R. A reappraisal of the morphology and systematic position of the theropod dinosaur *Sigilmassasaurus* from the "middle" Cretaceous of Morocco. *PeerJ* **3**, e1323 (2015).
32. Watanabe, A. *et al*. Vertebral pneumaticity in the ornithomimosaur *Archaeornithomimus* (Dinosauria: Theropoda) revealed by computed tomography imaging and reappraisal of axial pneumaticity in Ornithomimosauria. *PLoS One* **10**, e0145168 (2015).

33. Lü, J. *et al*. A new oviraptorid dinosaur (Dinosauria: Oviraptorosauria) from the Late Cretaceous of southern China and its paleobiological implications. *Sci. Rep.* **5**, 11490 (2015).
34. Lü, J. *et al*. High diversity of the Ganzhou oviraptorid fauna increased by a new "cassowary-like" crested species. *Sci. Rep.* **7**, 6393 (2017).
35. Lü, J. C. A new oviraptorosaurid (Theropoda: Oviraptorosauria) from the Late Cretaceous of southern China. *J. Vertebr. Paleontol.* **22**, 871 (2002).
36. Norell, M. A. & Makovicky, P. J. Important features of the dromaeosaur skeleton. II. Information from newly collected specimens of *Velociraptor*. *Am. Mus. Novit.* **3282**, 1 (1999).
37. Shen, C., Zhao, B., Gao, C.-L., Lü, J. & Kundrát, M. A new troodontid dinosaur, *Liaoningvenator curriei* gen. et sp. nov., from the Early Cretaceous Yixian Formation of western Liaoning Province, China. *Acta Geosci. Sin.* **38**, 1–13 (2017).
38. Shen, C. *et al*. A new troodontid dinosaur from the Lower Cretaceous Yixian Formation of Liaoning Province. *China. Acta Geol. Sin.* **91**, 763–780 (2017).
39. Osmólska, H., Currie, P. J. & Barsbold, R. In The Dinosauria. 2nd ed., Weishampel, D. B., Dodson, P. & Osmólska, H., Eds. (University of California Press, Berkeley), pp. 165–183 (2004).
40. Chiappe, L. M., Shu'an, J. & Qiang, J. Anatomy and systematics of the Confuciusornithidae (Theropoda: Aves) from the Late Mesozoic of Northeastern China. *Bull. Am. Mus. Nat. Hist.* **242**, 1 (1999).
41. Chiappe, L. M. & Walker, C. A. In *Mesozoic Birds: Above the Heads of Dinosaurs*, Chiappe, L. & Witmer, L. M., Eds (University of California Press), pp. 559–588 (2002).
42. Witmer, L. M. The craniofacial air sac system of mesozoic birds (Aves). *Zoological Journal of the Linnean Society* **100**, 327 (1990).
43. Müller, B. The air sacs of the pigeon. Smithsonian Miscellaneous. *Collections* **50**, 365 (1908).
44. Schwarz-Wings, D., Meyer, C. A., Frey, E., Manz-Steiner, H.-R. & Schumacher, R. Mechanics of pneumatic neck vertebrae in sauropod dinosaurs reveals a key role of vertebral pneumaticity for achieving enormous body sizes. *Proc. Roy. Soc. Lond. B* **277**, 11 (2010).
45. Fajardo, R. J., Hernandez, E. & O'Connor, M. P. Postcranial skeletal pneumaticity: A case study in the use of quantitative microCT to assess vertebral structure in birds. *J. Anat.* **211**, 138 (2007).
46. Erickson, G. M. *et al*. Was dinosaurian physiology inherited by birds? Reconciling slow growth in *Archaeopteryx*. *PLoS One* **4**, e7390 (2009).
47. Baumel, J. J. & Witmer, L. M. In *Handbook of Avian Anatomy: Nomina Anatomica Avium*, Baumel, J. J., King, A. S., Breazile, J. E., Evans, H. E. & Vanden Berge, J. C., Eds (Nuttal Ornithological Club, Cambridge, Massachusetts), pp. 45–132 (1993).
48. Bellairs, A. D. A. & Jenkins, C. A. In *Biology and Comparative Physiology of Birds*, Marshall, A. J., Ed. (Academic Press, New York), vol. 1, pp. 241–300 (1960).
49. Hogg, D. A. Fusions occurring in the postcranial skeleton of the domestic fowl. *J. Anat.* **135**, 501 (1982).
50. Storer, R. W. Fused thoracic vertebrae in birds: Their occurrence and possible significance. *J. Yamashina Inst. Ornithol.* **14**, 86 (1982).
51. James, H. F. Repeated evolution of fused thoracic vertebrae in songbirds. *The Auk* **126**, 862 (2009).
52. Kaiser, G. *The inner bird: Anatomy and Evolution*. (University of British Columbia) pp. 386 (2007).
53. Unwin, D. M. *Pterosaurs from Deep Time*. (Pi Press, New York 2006).
54. Witton, M. P. *Pterosaurs: Natural History, Evolution, Anatomy*. (Princeton University Press, Princeton, New Jersey), pp. 304 (2013).
55. Senter, P. Scapular orientation in theropods and basal birds, and the origin of flapping flight. *Acta Palaeont. Pol.* **51**, 305 (2006).
56. Longrich, N. R., Vinther, J., Meng, Q., Li, Q. & Russell, A. P. Primitive wing feather arrangement in *Archaeopteryx lithographica* and *Anchiornis huxleyi*. *Curr. Biol.* **22**, 2262 (2012).
57. Nudds, R. L. & Dyke, G. Narrow primary feather rachises in *Confuciusornis* and *Archaeopteryx* suggest poor flight ability. *Science* **328**, 887 (2010).
58. Feo, T. J., Field, D. J. & Prum, R. O. Barb geometry of asymmetrical feathers reveals a transitional morphology in the evolution of avian flight. *Proc. Roy. Soc. Lond. B* **282**, 20142864 (2015).
59. Cubo, J. & Casinos, A. Incidence and mechanical significance of pneumatization in the long bones of birds. *Zool. J. Linn. Soc. Lond.* **130**, 499 (2000).
60. Currey, J. D. & Alexander, R. M. The thickness of the walls of tubular bones. *J. Zool. Lond.* **206**, 453 (1985).

Acknowledgements

We thank Elke Siebert (MfN) for her help with scanning photographs, and the preparators Lutz Berner and Markus Brinkmann for their assistance in handling the Berlin *Archaeopteryx*. We are grateful to Peter J. Makovicky and two other anonymous referees for their valuable comments and hints on earlier versions of this manuscript. MK was supported by Scientific Grant Agency VEGA of the Ministry of the Education, Science, Research and Sport of the Slovak Republic (1/0853/17). GD acknowledges support from UEFISCDI Romania [grant number PN-III-P4-ID-PCE-2016-0572]. The publication of this article was funded by the Open Access Fund of the Leibniz Association.

Author Contributions

D.S. and M.K. designed and performed the research; D.S., M.K., H.T., G.D. and R.C. contributed analytical tools and comparative data and/or discussed the manuscript during progress; D.S. and M.K. analyzed data; D.S., M.K., G.D. and R.C. wrote the paper.

Additional Information

Supplementary information accompanies this paper at https://doi.org/10.1038/s41598-019-42823-5.

Competing Interests: The authors declare no competing interests.

Publisher's note: Springer Nature remains neutral with regard to jurisdictional claims in published maps and institutional affiliations.

Supplemental Information to

Ultraviolet light illuminates the avian nature of the Berlin *Archaeopteryx* skeleton

Daniela Schwarz[1*], Martin Kundrát[2*], Helmut Tischlinger[3], Gareth Dyke[2,4], Ryan M. Carney[5]

[1] Museum für Naturkunde, Leibniz Institute for Evolution and Biodiversity Science, 9115 Berlin, Germany.

[2] Center for Interdisciplinary Biosciences, Technology and Innovation Park, University of Pavol Jozef Šafárik, 04154 Košice, Slovakia.

[3]Tannenweg 16, 85134 Stammham, Germany.

[4] Department of Geology, Babes-Bolyai University, Romania.

[5] Department of Integrative Biology, University of South Florida, 33620 Tampa, FL, USA.

Vertebral Position	**Unambiguous pneumatic structures: pneumatic foramina (pf), internal pneumatic camerae (ipc), camellae (cam)**	**Ambiguous pneumatic structures: small pores of similar size and regular distribution(abs), irregularly distributed small rounded putative camellae (amf)**	**Putative nutrient foramina**	**Pneumatizing air sac[1]**
Presacral 2, Axis (Fig. 1)	high oval pf posteriorly at lateral face vertebral body	none	small foramen at lamina of prezygapophysis	cervical air sac
Presacral 3, 3rd Cervical (Fig. 1)	long oval pf ventrally at lateral face of vertebral body, pf at lateral face of vertebral body and pf ventral to praezygapophysis, rounded rectangular camellae at neural arch and neural spine	fossa in dorsal half of lateral vertebral body; abraded lateral surface of vertebral body reveals abs; amf along lateral face of prezygapophysis; bone abrasion reveals abs at head of cervical rib	none	cervical air sac
Presacral 4, 4th	long oval pf at lateral face of vertebral body	abraded bone exposes pattern of abs filling	none	cervical air sac

Cervical, (Fig. 1)		vertebral body and neural arch and spine		
Presacral 5, 5th Cervical (Fig. 1)	two rounded pf in rostral half of lateral face of vertebra body, one pf in posterior half of lateral face of vertebral body	two fossae visible laterally at vertebral body; abs visible at lateral vertebral body anteriorly and around pneumatic foramen and at neural spine	none	cervical air sac
Presacral 6, 6th Cervical (Fig.1)	long oval pf at lateral face of vertebral body, rounded angular camellae at lateral face of vertebral body and base of neural arch along a line connecting pre- and postzygapophysis	neural canal shows a pattern of rounded rectangular voids that might be camellae; abs at abraded lateral surface of neural spine and at cervical rib head with spongy bone	none	cervical air sac
Presacral 7, 7th Cervical (Fig. 1)	fragment of neural arch reveals camellae	problematic bone fragment at vertebral body that might have been added during preparation[2], not included into observation here	none	cervical air sac
Presacral 8, 8th Cervical (Fig. 2)	interior of vertebral body hollowed out by ipc in its central two-thirds; camellae visible at lateral neural arch	abraded lateral surface in posterior half of vertebral body with abs, cervical rib head with amf		cervical air sac
Presacral 9, 9th cervical (Fig. 2)	interior of vertebral body hollowed out by ipc in its central two-thirds; abraded bone in posterior part of lateral vertebral body exposes camellae	Abraded lateral surface of vertebral body (anteriorly) and neural arch (posteriorly) exposes abs	none	cervical air sac
Presacral 10, 10th cervical (Fig. 2)	interior of vertebral body hollowed out by ipc in its anterior half; another pneumatic cavity ventrally; 2 unambigous camellae at lateral face of vertebral body posterior to ipc	Abraded lateral surface of vertebral body exposes abs around ipc; fossa laterally at neural arch	Lateral face of neural arch with two foramina	cervical air sac
Presacral 11, 1st thoracic (Fig. 2)	interior of vertebral body hollowed out by ipc in its central two-thirds; ipc ventral to diapophysis; camellae on neural arch dorsal to diapohysis	Abraded lateral surface of vertebral body, diapophysis and lateral face of prezygapophysis exposes abs, oval fossa at neural arch between diapophysis and prezygapophysis	none	cervical air sac
Presacral 12, 2nd	interior of vertebral body hollowed out by ipc in its central two-thirds; ipc	abraded cortical bone on lateral vertebral body exposes abs; canal like	none	cervical air sac or pulmonary

thoracic (Fig. 2)	ventral to diapophysis; dorsal face of diapophysis with abraded cortical bone exposing camellae and combined with pf with aperture in lateral neural spine, camellae continue posteriorly along the prezygapophysis of the 13th presacral vertebra	hollow area at base of postzygapophysis; neural arch dorsal to postzygapophysis laterally abraded exposing spongy internal bone structure; rostral part of lateral neural arch exposes amf		diverticula of lung
Presacral 13, 3rd thoracic (Fig. 2)	vertebral body medially with 2 narrow and elongate ipc, anterior and posterior to diapophysis each a large ipc, rounded pf or ipc ventral to prezygapophysis; large pneumatic cavities under diapophysis	ventral two-thirds of lateral vertebral body and anterior part of neural arch base and vertebral body with abs; lateral face of neural spine exposes amf	none	cervical air sac or pulmonary diverticula of lung
Presacral 14, 4th thoracic (Fig. 2)	ipc ventral at prezygapophysis; camellae at base of neural spine along a lamina from pre- to postzygapophysis	Dorsal half of lateral vertebral body with abs and deep preservational cavity; surface of diapophysis and base of neural arch ventral to neural canal covered with pattern of amf; lateral face of neural spine exposes large opening that might be either pneumatic foramen or preservational	Lateral face of neural spine with a number of small circular foramina	cervical air sac or pulmonary diverticula of lung
Presacral 15 (Fig. 2)	none	dorsal half of lateral vertebral body laterally with abs; most of neural arch is crushed; abs visible at prezygapophysis, base of neural spine and apical region of neural spine	two small foramina in ventral half of lateral face of vertebral body	cervical air sac or pulmonary diverticula of lung
Presacral 16 (Fig. 2)	In anterior half of lateral face of vertebral body drop shaped and sharply bounded pf; long-oval pf medially at lateral face of neural arch; rectangular camellae hollow out postygapophysis	Lateral face of vertebral body and region ventral to postzygapophysis exposes abs with regionally larger hollows that might be camellae; two fossae laterally at prezygapophysis	small foramina lie within neural canal and at base of neural arch posterior to pneumatic foramen	cervical air sac or pulmonary diverticula of lung
Presacral 17 (Fig. 2)	none	remnant of possible foramen visible at anterior part of lateral	none	Probably abdominal air sac

		vertebral body; lateral surface of vertebral body, base of neural arch and lateral surface of prezygapophysis with abs; lateral surface of vertebral body medially with small, irregular foramina that might be preservation-related resorption traces; large bowl-shaped fossa visible ventrally to postzygapophysis at caudolateral part of neural arch		
Presacral 18 (Fig. 2)	none	oblique and oval fossa or foramen at lateral face of vertebral body; distinct long-oval fossa at lateral face of neural arch base, anteriorly followed by a narrow and triangular fossa, and a deep long oval fossa at lateroventral face of prezgyapophysis; irregular foramina that might be preservation-related resorption traces visible at vertebral body; abraded surface exposes abs at lateral face of vertebral body	foramen anteriorly at prezygapophysis	abdominal air sac
Presacral 19 (Fig. 2)	Combination of elongate fossa with a narrow pf in anterior half of lateral vertebral body and at base of neural arch ventral to postzygapophysis	Lateral surface of vertebral body and base of neural arch with abs; lateral surface of neural spine eroded and exposes amf	putative foramen (or result of erosion of bone) visible laterally at neural spine	abdominal air sac
Presacral 20 (Fig. 2)	Abraded bone surface exposes camellate internal bone structure at lateral side of postzygapophysis and neural arch base	Elongate fossa visible at lateral face of vertebral body, obliquely oriented oval shaped fossa at lateral side of neural arch; lateral side of vertebral body exposes anteriorly and posteriorly abs; neural arch at base along prezygapophysis and along lateral face of neural spine with amf	none	abdominal air sac

Presacral 21 (Fig. 2)	none	small, elongate, slitlike putative fossa in anterior third of lateral vertebral body; lateral face of vertebral body exposes abs; amf exposed at lateral face of neural spine	none	abdominal air sac
Presacral 22 (Fig. 3A)	large, elongate sharp lipped pf in posterior two-thirds of vertebral body	fossa dorsal to pf at lateral face of vertebral body; abs visible in anterior part of lateral face of vertebral body and along an area at neural arch connecting pre- and postzygapophysis		abdominal air sac
Thoracic ribs (Fig. 2)	none	abs exposed at heads and along shaft of ribs on 12^{th}, 13^{th}, 14^{th}, 15^{th}, 16^{th}, 18^{th}, 19^{th}, 20^{th} and 21^{st} presacral vertebrae, all thoracic ribs are broken and expose only thin bone walls with strongly hollowed out shafts	none	abdominal air sac
Sacral vertebra 1 (Fig. 3A)	none	abs anteriorly and posteriorly at lateral face of vertebral body, canal like structure with foramina at anterior part of base of neural arch	foramen at medial face of vertebral body, 2 foramina at anterior half of neural arch around prezygapophysis	abdominal air sac
Sacral vertebra 2 (Fig. 3A)	none	small part of vertebral body visible, abraded bone exposes abs	none	abdominal air sac
Caudal vertebra 1 (Fig. 3A)	large irregular ipc in anterior and posterior half of vertebral body	abs is exposed in anterior half of lateral vertebral body and at base of neural arch	foramen at ventral part of neural arch, two foramina at anterior margin of haemapophysis	abdominal air sac
Caudal vertebra 2 (Fig. 3A)	elongate ipc laterally at vertebral body, vertebral body and neural arch filled with camellae	none	none	abdominal air sac
Caudal vertebra 3 (Fig. 3A)	rounded ipc in anterior and posterior half of lateral vertebral body	lateral face of vertebral body and base of neural arch expose amf	none	abdominal air sac

Caudal vertebra 4 (Fig. 3A)	none	Posterior third of vertebral body, and lateral face of neural arch with abs; putative camellae at base of neural arch	none	abdominal air sac
Caudal vertebra 5 (Fig. 3A, 3C)	camellae at base of neural spine	area with abs at vertebral body and haemapophysis	none	abdominal air sac
Caudal vertebra 6 (Fig. 3C)	camellae along postzygapophysis	abs and amf anteriorly and posteriorly visible at vertebral body and neural arch	foramen in caudal part of lateral vertebral body	abdominal air sac
Caudal vertebra 7 (Fig. 3C)	none	abs and amf at lateral vertebral body and neural arch	none	abdominal air sac
Caudal vertebra 8 (Fig. 3C)	none	small areas with amf and abs are visible at lateral vertebral surface	narrow and slit-like foramina at base of neural arch	abdominal air sac
Caudal vertebra 9 (Fig. 3C)	none	abs at base of neural spine, large sharp lipped foramen occupies medial part of lateral vertebral centrum - this is plausibly interpreted to breakage structure	none	abdominal air sac
Caudal vertebra 10 (Fig. 3D)	none	amf at base of neural spine, large sharp lipped foramen occupies anterodorsal part of lateral vertebral centrum - this is plausibly interpreted to breakage structure	foramen at base of postzygapophysis	abdominal air sac
Caudal vertebra 11 (Fig. 3D)	camellae are visible in anterior half of vertebral body and embedded in pattern of abs, camellae at postzygapophysis	lateral face of vertebral body exposes abs	none	abdominal air sac
Caudal vertebra 12 (Fig 3D)	small rounded and internconnected ipc are visible laterally at vertebral body	lateral face of neural arch exposes abs	none	abdominal air sac
Caudal vertebra 13 (Fig. 3D)	None	none	none	abdominal air sac
Caudal vertebra 14 (Fig. 3D, E)	vertebral body is internally hollowed out by 2 elongate cavities interpreted as ipc	none	two foramina at base of neural arch	abdominal air sac

Caudal vertebra 15 (Fig. 3D, E)	vertebral body is internally hollowed out by 2 elongate cavities interpreted as ipc	none	none	abdominal air sac
Caudal vertebra 16 (Fig. 3E)	vertebral body is internally hollowed out by narrow ipc	none	none	abdominal air sac
Caudal vertebra 17 (Fig. 3E)	none	none	foramen anteriorly at lateral face of neural spine	abdominal air sac
Caudal vertebra 18-20 (Fig. 3E)	none	none	none	abdominal air sac
Humerus (Fig. 2)	None	none	proximal extremity bears five foramina distributed along margins, dorsal part of deltopectoral crest with large break at rounded foramen	clavicular and cranial thoracic air sac
Ilium (Fig. 3A)	none	posterior iliac process with laterally abraded bone exposing abs, small area with amf slightly rostrally to abs at posterior iliac process; narrow zone of abs cranioventrally at iliac margin	Several foramina are positioned along posterior half of iliac blade and pubic process, dorsal margin bears two putative foramina	abdominal air sac
Pubis (Fig. 3A)	none	abs exposed at pubic head	small foramina posteriorly at pubic head and along anterior margin of proximal shaft	abdominal air sac
Ischium (Fig. 3A)	none	none	foramen at ischium shaft	abdominal air sac
Femur	none	none	medial foramen on distal shaft and at mid-shaft height	abdominal air sac
Tibia	none	none	foramina at mid-shaft height	abdominal air sac

Table S1. Details of pneumatic structures observed in the postcranial skeleton of the Berlin specimen of *Archaeopteryx*, MB.Av.101, with references to figures. The presacral vertebral count of the Berlin specimen is taken in accordance with Britt et al.[3]

Specimen	**Femur length**	**Observed pneumatic features**
Eichstätt specimen	37.0 mm	Ambiguous: cervical vertebra with laminae and fossae, possibly pneumatic foramen in anterior thoracic vertebra[3].
Munich specimen	48.0 mm	Ambiguous: cervical vertebrae preserve some laminae, mention of a pneumatic foramen in a posterior thoracic by Elzanowski[4].
Thermopolis specimen	50.3 mm[5]	Unambiguous: X-ray figure in Mayr et al.[5] shows camellae within cervical vertebrae.
Berlin specimen	52.6 mm	Unambiguous: UV images show continuous pattern of pneumatic camellae throughout the whole vertebral column and pelvis. Pneumatic foramina in cervical vertebrae as documented by Britt et al.[3] and O'Connor[6]
12th specimen	~53 mm[7]	Unambiguous: intraosseous pneumatic structure in mid-cervical vertebra and 8th cervical vertebra, pneumatic foramen in 1st thoracic vertebra[7]
11th specimen	55.3 mm[8]	Ambiguous: cervical and anterior thoracic vertebrae seem to show laminae and fossae[8].
Maxberg specimen	56.4 mm	X-ray photographs and figure of lumbar and anterior thoracic vertebra in Wellnhofer[2] exposes internal pneumaticity of anterior thoracic and posterior thoracic vertebrae (with hiatus between), centered around neural arch.
London specimen	61.0 mm	Ambiguous: pneumatic foramen in pubis and anterior thoracic vertebral centrum reported by

		Christiansen and Bonde[9], earliest report of camellate pneumatic bone by Owen[10]
Solnhofen specimen	67.0 mm	Poor preservation[2] prevents evaluation of pneumatization status.

Table S2. List of *Archaeopteryx* specimens with preservation of vertebral pneumaticity.

Femur lengths are taken from Wellnhofer[2] unless otherwise noted.

O'Connor 2004[1] (n=17)	O'Connor 2009[11] (n=12)	This study (n=18)
Composite units		
CRC, Cranial Cervical Vertebrae* **MC**, Middle Cervical Vertebrae* **CAC**, Caudal Cervical Vertebrae*	**CeV**, cervical vertebrae	**ANC**, Anterior Cervical Vertebrae **MC**, Middle Cervical Vertebrae **POC**, Posterior Cervical Vertebrae
CRT, Cranial Thoracic Vertebrae **CAT**, Caudal Thoracic Vertebrae	**TV**, thoracic vertebrae	**ANT**, Anterior Thoracic Vertebrae **POT**, Posterior Thoracic Vertebrae
SS, Synsacral Vertebrae	**SV**, sacral vertebrae	**SS**, Synsacral Vertebrae
CA, Caudal Vertebrae	**CaV**, caudal vertebrae	**CAA**, Anterior Caudal Vertebrae **CAP**, Posterior Caudal Vertebrae
VR, Vertebral Ribs **SR**, Sternal Ribs	**CO**, costal elements	**TR**, Thoracic Ribs N/A **CAR**, Caudal Ribs and Chevrons
CX, Fused Ilium-Ischium-Pubis	**Plv**, pelvic girdle elements	**PE**, Pelvis (Ilium, Ischium, Pubis)
DLE, Distal Limb Segments**	**DFL**, distal forelimb elements **DHL**, distal hind limb elements	**DFL**, distal forelimb elements** **DHL**, distal hind limb elements**
Individually scored units		
CC, coracoids **SC**, scapulae **FU**, furculae	**Pct**, pectoral girdle elements	**CC**, coracoids **SC**, scapulae **FU**, furculae
ST, sterna	**ST**, sternum	N/A
HU, humeri	**Hu**, humerus	**HU**, humeri
FM, femora	**Fe**, femur	**FM**, femora

*Cervical ribs were scored with their respective vertebrae, as they are fused in extant birds.
** Distal Limb Elements = bones distal to elbow or knee joints

Table S3. Differences between the Anatomical Units (AUs) and acronyms used in this study and by O`Connor[1,11].

Supplementary references

1. M. P. O'Connor. Pulmonary pneumaticity in the postcranial skeleton of extant aves: a case study examining Anseriformes. *J. Morphol.* **261**, 141 (2004).

2. P. Wellnhofer. *Archaeopteryx. Der Urvogel von Solnhofen*. (Verlag Dr. Friedrich Pfeil, München, 2008), pp. 256.

3. B. B. Britt, P. J. Makovicky, J. Gauthier, & N. Bonde. Postcranial pneumatization in Archaeopteryx. *Nature* **395**, 374 (1998).

4. A. Elzanowski. in *Mesozoic Birds: Above the Heads of Dinosaurs,* L. Chiappe, L. M. Witmer, Eds. (University of California Press, 2002), pp. 129-159.

5. G. Mayr, B. Pohl, S. Hartman, & D. S. Peters. The tenth skeletal specimen of *Archaeopteryx*. *Zool. J. Linn. Soc.* **149**, 97 (2007).

6. M. P. O'Connor. Postcranial pneumaticity: An evaluation of soft-tissue influences on the postcranial skeleton and the reconstruction of pulmonary anatomy in archosaurs. *J. Morphol.* **267**, 1199 (2006).

7. O. W. M. Rauhut, C. Foth, & H. Tischlinger. The oldest *Archaeopteryx* (Theropoda: Avialae): a new specimen from the Kimmeridgian/Tithonian boundary of Schamhaupten, Bavaria. *PeerJ* **6:e4191** (2018).

8. C. Foth, H. Tischlinger, & O. W. M. Rauhut. New specimen of *Archaeopteryx* provides insights into the evolution of pennaceous feathers. *Nature* **511**, 79 (2014).

9. P. Christiansen & N. Bonde. Axial and appendicular pneumaticity in *Archaeopteryx*. *Proc. Roy. Soc. Lond., Ser. B* **267**, 2501 (2000).

10. R. Owen. On the *Archaeopteryx* of von Meyer, with a description of a new long tailed species from the lithographic stone of Solenhofen. Philosophical Transactions of the Royal Society of London **153**, 33 (1864).

11. M. P. O'Connor. Evolution of Archosaurian body plans: skeletal adaptations of an air-sac-based breathing appartus in birds and other archosaurs. *J. Exp. Zool.* **311A**, 629 (2009).